Stratigraphic Model of East Biak Based on Magnetotelluric Data

Alviyanda[1*], Gusti Muhammad Lucki Junursyah[2] & Prihadi Sumintadireja[3]

[1]Geological Engineering Study Program, Institut Teknologi Sumatera,
Jalan Ryacudu, Jati Agung, Lampung Selatan 35365, Indonesia
[2]Center for Geological Survey, Geological Agency,
Jalan Diponegoro No. 57, Bandung 40122, Indonesia
[3]Research Division of Applied Geology,
Geology Department-Faculty of Earth Sciences and Technology,
Institut Teknologi Bandung, Ganesha No. 10, Bandung 40132, Indonesia
*E-mail: alviyanda@gl.itera.ac.id

Abstract. Biak Island is thought to have originated from the Australian Continental passive margin in the Mesozoic. This passive margin underwent tectonic collision to form the bedrock of Biak Island during the Paleogene. East Biak is covered by limestone, which is an obstacle to knowing the deeper stratigraphy. This study's aim was to identify the subsurface geology of the East Biak area based on rock resistivity values. Magnetotelluric (MT) surveying is a passive geophysical method that is able to interpret subsurface geology based on rock resistivity values at depths of up to 5 to 10 km. The MT measurements in East Biak used 25 measurement points. Cross-sectional variations in rock resistivity values generated from the MT measurements were used to identify rock types in the East Biak subsurface. Five rock units were identified. The East Biak stratigraphy model is dominated by carbonates, comprising two sequences, i.e. an Early Neogene sequence with a thickness of 1,000 to 3,000 m and a Late Neogene to Quaternary sequence with a thickness of 180 to 2,450 m. The unconformity between these two sequences is due to tectonic activity, which separated Supiori and Biak Island.

Keywords: *East Biak; magnetotellurics; resistivity; stratigraphic model; unconformity.*

1 Introduction

Biak Basin is a Tertiary basin between the Australian Continental and the Pacific Oceanic Plate. During the Paleogene, the northern part of the Australian Plate collided with the island arc when approaching the subduction zone to the north under the Pacific plate (Dewey and Bird [1], Milsom, *et al*. [2], Hall [3], and Cloos, *et al*. [4]), which formed the bedrock of Biak Island and its basin. The Biak Basin is located south and east of Biak Island, which is covered by coral limestone.

Received February 4th, 2019, 1st Revision April 13th, 2020, 2nd Revision June 15th, 2020, Accepted for publication June 17th, 2020.

DOI: 10.5614/j.math.fund.sci.2020.52.2.7

The research area is located in East Biak, which is the boundary of the Biak Basin according to the Geological Agency of Indonesia. East Biak's geomorphology has the characteristic of karst with the existence of an underground river that flows to the sea. The presence of coral limestone and chalky limestone that covers almost the entire surface of East Biak is an obstacle to knowing the deeper stratigraphy and structure.

Magnetotelluric (MT) surveying is a passive geophysical method capable of interpreting subsurface geology based on variations in rock resistivity at depths of up to 5 to 10 km. This method has advantages in its use in the field: it is environmentally friendly, it can be used in areas with a steep relief, and it is mobile. The subsurface geology can be seen from the cross-section interpretation of 1D and 2D MT models correlated with the regional geology.

2 Geological Setting

New Guinea is part of the northern boundary of Australia that has collided with an island arc (Hall [3], Hill and Hall [5], and Gold, *et al.* [6]). The boundary between this collision includes major structures such as the Sorong Fault, Ransiki Fault, which continues to Cendrawasih Bay, and Tanjung Wandeman in the east, which is connected with the Weyland overthrust [6], as shown in Figure 1.

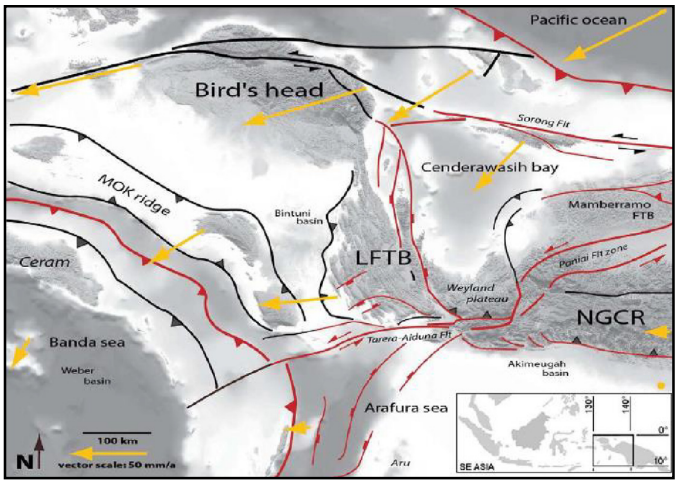

Figure 1 Simplified regional maps (terrestrial Shuttle Radar Topography Mission – SRTM – and bathymetry prediction), with the main plate boundaries and faults indicated by black lines, active structures by red lines, and GPS data by yellow lines, relative movements to the Australian Plate according to Bailly, *et al.* [7].

In the Late Cretaceous, rifting activity occurred to the north of New Guinea, forming a new oceanic crust before the Eocene [3,5]. In the Eocene to Late Oligocene, volcanic activity formed the Philippine island arc from subduction zones to the north. In the Early Miocene, along with the plate movement of the Pacific and Caroline plates, subduction events caused the volcanic activity to stop due to collisions between the island arc and the continent. Evidence in the field of this collision is the outcrop of serpentinized ultramafic rocks at the surface. In the Late Miocene to Late Pleistocene, the entire Biak Island again subsided slowly and continuously. This stopped when there was a reversal. Later, uplift occurred relatively slowly, which continues to this day, as evidenced by the presence of several carbonate highs.

There are two main regimes that affect Biak Island based on the geological conditions on the surface and Bouguer Anomaly maps based on Saragih, *et al*. [8]. The regimes are transtensive and pure strike-slip. Both of these regimes influenced the formation of Biak Island and sediment deposition. The rifting and uplifting phenomena of the two regimes are based on the minimum horizontal stress σ3 from the relative magnitude of the horizontal stress, which forms an extensive-transtensive stress regime, and the maximum horizontal stress σ1 from the relative magnitude of the horizontal stress, which forms a compressive-transpressive regime.

Based on the geological map of the Biak quadrangle, Irian Jaya (1:250,000) by Masria, *et al*. [9] it is known that the research area consists of several formations from old to young, as follows (Figure 2):

1. Korido formation(s), consisting of phyllite, quartzite, flint, tufa, greywacke, and sandstone. This unit is intruded by a small basalt dyke.
2. Auwewa formation (Teoa), consisting of volcanic rocks; they are lava and tuff, locally at the bottom of the insertion breccia and conglomerate. On Biak Island, serpentinized peridotite and gabbro are found, along with basalt. The formations were deposited in the Eocene until the Early Oligocene.
3. Wainukendi formation (Tomw), consisting of crystalline limestone, medium to coarse-grained, local conglomerate lenses and marl intercalations and limestone. This formation was deposited in the Late Oligocene to the Early Miocene, a neritic environment and has conformably overlies or has an interfingering relationship with a Wafordori formation.
4. Wafordori formation (Tmw), consisting of marl and some tuffs; thinly inserted with sandstone and crystal limestone. This formation is deposited in a littoral to neritic environment and is conformably overlain by a Napisendi formation.

5. Napisendi formation (Tmn), consisting of layered limestone, fine-grained tuffaceous clastic limestone to rough and slightly solid limestone; intercalated with conglomerates, breccias, sandy limestone, and marl. This formation is unconformably overlain by younger formations.
6. Korem formation (Tmk), consisting of marl and chalky marl; intercalated with local sandy marl and marly limestone. This formation has an interfingering conformity with rocks above it.
7. Wardo formation (Tmpw), consisting of marly limestone and sandy limestone with the presence of small foraminifera; at the top it consists mainly of limestone. This formation is conformably overlain by younger rock.
8. Mokmer formation (Qm), consisting of coral limestone at the top and chalky limestone at the bottom. The limestone contains fossils of planktonic foraminifera, coral fragments, algae, and molluscs.

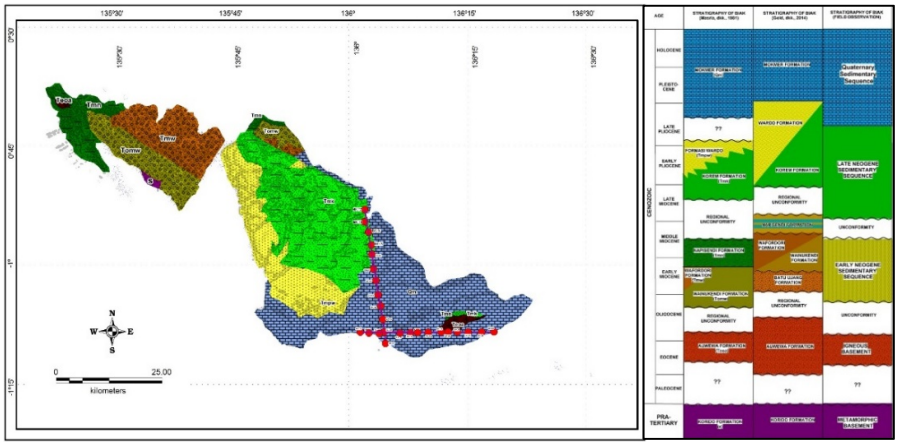

Figure 2 Geological map of Biak Island and its surroundings (with MT measurement points), and comparison of Biak stratigraphic columns according to Masria, *et al.* [9], Gold, *et al*. [6] and field observation.

3 Method

The data used in this study were based on observations of outcrops in the field and magnetotelluric surveying. The observations of outcrops performed included descriptions of rock by conducting petrographic and micropaleontologic analysis so that they could be grouped based on rock depositional facies. The stratigraphic model of the research area was obtained from the correlation between rock depositional facies and the regional geology.

The MT survey was conducted using Phoenix MTU-5A equipment to determine the subsurface geology of the research area. MT measurements were performed in East Biak, using two lines with a total of 25 measurement points with west-east and south-north directions based on Junursyah [10] and Junursyah, *et al.* [11]. One-dimensional inversion modeling was performed using Occam's inversion by dividing the total layer into 8 layers based on vertical variations in resistivity up to a depth of 10 km (Figure 3). Two-dimensional inversion modeling was done in Smooth Model Inversion along both lines.

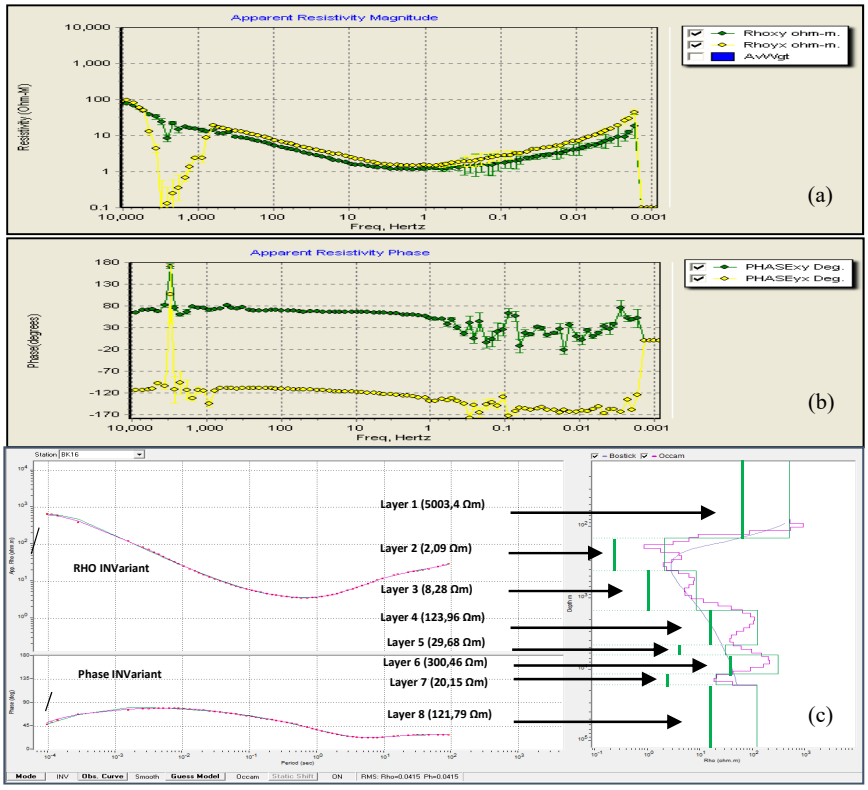

Figure 3 Example of data processing result at the measurement point of BK-25 (a & b) apparent resistivity and phase curve limited to 10 km of depth: (c) inversion modelling with up to eight layers resistivity variation.

The stratigraphic correlation of the general variation of rock resistivity (Table 1) according to Alviyanda, *et al*. [12] produced a stratigraphic model based on the rock resistivity values in the study area (Table 2). The pattern of resistivity variation in each rock formation shows the comparability layers based on MT soundings at each measurement point.

The comparability results show the distribution of layers based on vertical variations in resistivity. The 2D model analysis was carried out by correlating the 1D model and rock distribution on the surface and their continuity to identify the lateral rock distribution. Discontinuities can be identified as geological anomalies in the form of geological structures. The correlation between the 2D model and the geological surface data produced subsurface geological models and geological structures (Figure 4).

Table 1 General resistivity values of rock according to Alviyanda, *et al.* [12].

ROCK	DESCRIPTION	RESISTIVITY (ohm.m) min	RESISTIVITY (ohm.m) max
WATER	Sea water	0.3	1
	Fresh Water	10	100
	Acid Water	20	100
SOIL	Aluvium	7.5	850
	Top Soil	150	900
	Gravel	100	3,200
SEDIMENT	Clay/lapili	1	100
	Shale/lapili	20	2,000
	Sandstone/tuff	28	4,500
	Conglomerate/aglomerate	2,000	10,000
META	Argilite	10	900
	Schist	10	10,000
	Slate	500	500,000
	Quarzite	500	800,000
CARBONATE	Marls	5	100
	Chalk	50	150
	Dolomit	350	10,000
	Limestone	50	300,000
COAL	Lignite	10	200
	coal	100	700
IGNEOUS	Lava	100	50,000
	Basalt-Gabro	1,000	1,000,000
	Andesite-Diorite	3,000	40,000
	Ryolite-Granite	5,000	1,000,000
META	Gneiss	68,000	3,000,000

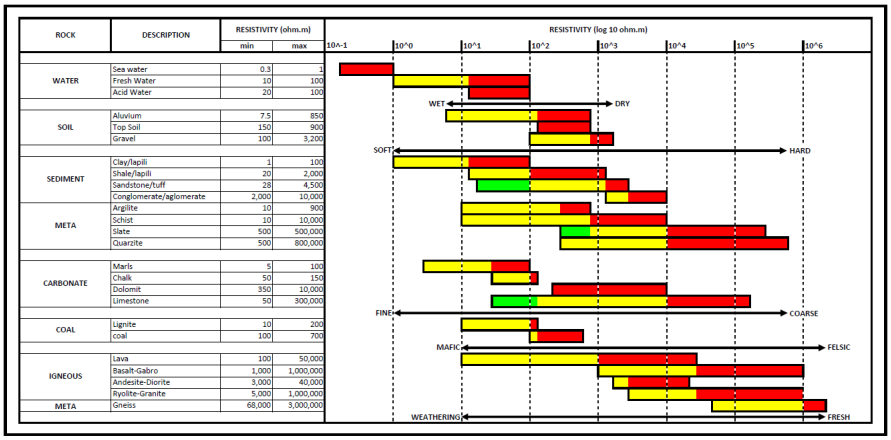

Table 2 Stratigraphic model based on rock resistivity values in Biak and surrounding areas correlated with the regional stratigraphy according to Masria, *et al*. [9] and field observation of sedimentary sequences.

FORMATION		AGES	THICK (m)	COMPONENT	AVERAGE (Ωm) MIN	AVERAGE (Ωm) MAX	AVERAGE (Ωm)	Field Observation
Qm	Mokmer Formation	Pleistocene - Holocene	± 250 m	coral limestone chalk	100	150075	75088	Quaternary Sedimentary Sequence
Tmpw	Wardo Formation	Late Miocene - Pliocene	± 250 m	chalk marly limestone marly	20	100067	50043	Late Neogene Sedimentary Sequence
Tmk	Korem Formation	Late Miocene	± 300 m	marl inserts limestone chalk marl marl	5	2563	1284	
Tmn	Napiendi Formation	Early Miocene	500-600 m	layering limestone tuffaceous limestone solid limestone conglomerate breccia sandy limestone marl fine-caorse sandstone	473	56538	28506	Early Neogene Sedimentary Sequence
Tmw	Wafordori Formation	Early Miocene	± 600 m	crystal limestone marl inserts sandstone tuffaceous marl marl	41	76013	38027	
Tomw	Wainukendi Formation	Late Oligocene - Early Miocene	500-600 m	crystal limestone limestone lens conglomerate clastic limestone limestone inserts marl	2576	82500	42538	
Teoa	Auwewa Formasi	Eocene - Early Oligocene	< 200 m	lava conglomerate breccia serpentinized peridotite gabbroic basalt	17502	678500	348001	Igneous Basement
s	Koridо Formation	Pra-Tertiary	?	phyllite quartzite chert meta-tuffaceous basalt crack	506	15080	7793	Metamorphic Basement

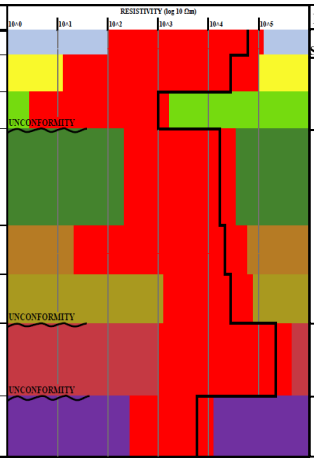

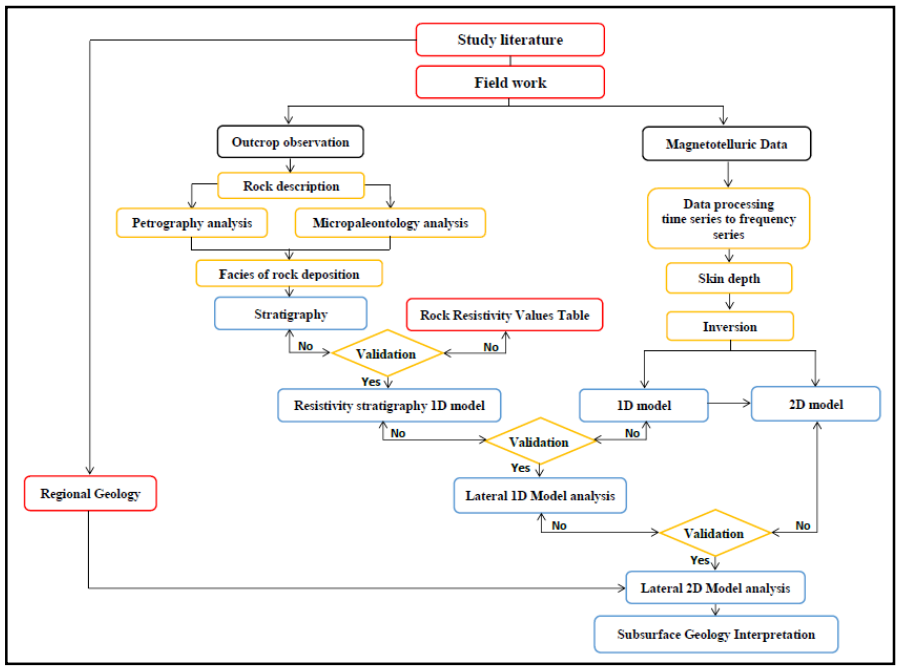

Figure 4 Flowchart of research methods used, from fieldwork, data processing, modeling, and stratigraphic models to subsurface geological interpretation.

4 Result and Analysis

4.1 Stratigraphic Research Areas

Based on observations of the surface geology conducted on Biak and Supiori Island, the study area was divided into five main units, i.e. Metamorphic Basement Supiori Island, Igneous Basement Biak Island, Early Neogene sequence, Late Neogene sequence and Quaternary sequence. Correlation of rock units was performed using the composite log of the track traversed in Biak and Supiori Island, which was correlated with the regional geology (Figure 5). The Metamorphic Basement Supiori Island consists of phyllite, schist, and gneiss, and has a foliation with a strong joint density and is filled with quartz veins. This unit is bedrock found on Supiori Island, comparable with the Korido Formation; it is Pre-Tertiary according to Masria, *et al*. [9]. The Igneous Basement Biak Island consists of peridotite, serpentinite, diabase and some volcanic rocks like breccia and tuff. These two latter rock units are Eocene bedrock on Biak Island, comparable with the Auwewa Formation according to Masria, *et al.* [9].

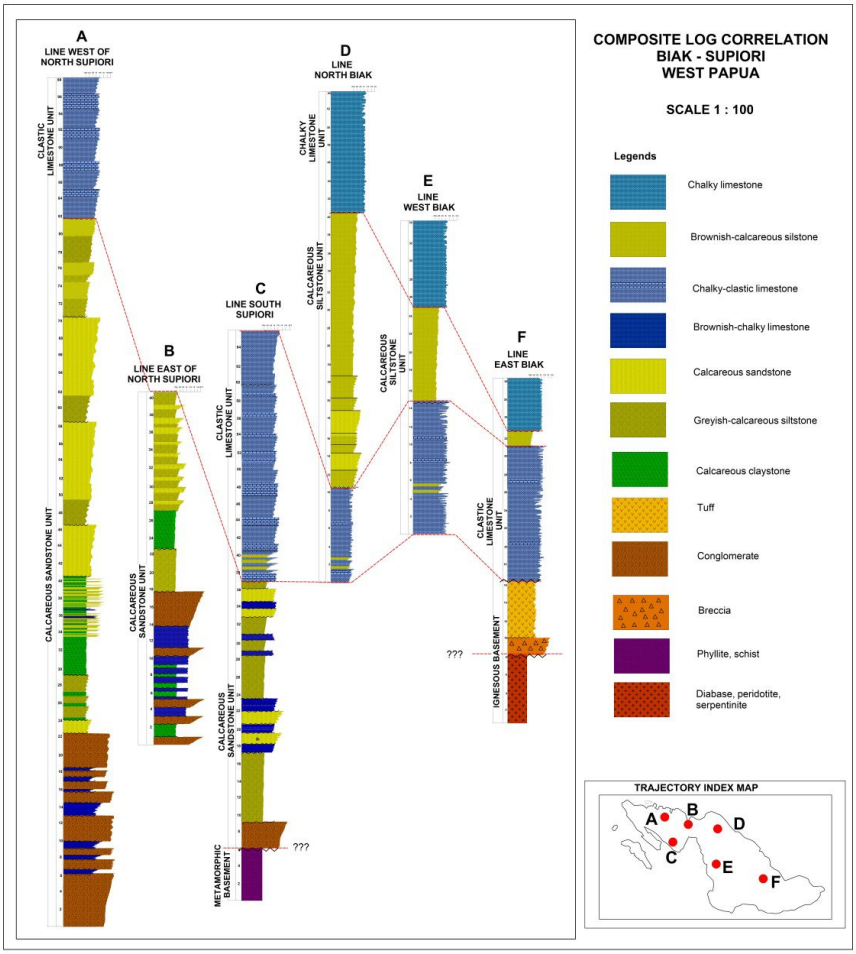

Figure 5 Composite log observations on Biak and Supiori Islands.

The existence of two lithologies that are genetically different on the surface is thought to have been influenced by tectonic activity. According to Gold, *et al.* [6], the convergent boundary between the oceanic crust north of the Australian continent and the Caroline island arc produced volcanic activity. At the end of the subduction, the collision of the Australian continent and the Caroline island arc resulted in the shifting of oceanic crustal rock on the surface of Biak Island in the Late Oligocene.

The sedimentary rock is divided into three sequences: Early Neogene, Late Neogene and Quaternary. The lower Early Neogene sedimentary sequences

consist of calcareous claystone, greyish calcareous siltstone, boundstone-grainstone-limestone based on Dunham [13], while at the bottom there are calcareous claystone, chalky limestone and massive conglomerates. These rock units are comparable with the Wainukendi and Wafordori formations. The upper Early Neogene sedimentary sequences consist of limestone grainstone and boundstone based on Dunham [13]. Limestone bioclasts are dominated by coral, both tabular and domal, and there are fossils of shells with a size of >1 cm. This unit is comparable with the Napisendi Formation according to Masria, *et al.* [9]. Both of these rock units have a conformable and interfingering stratigraphic relationship.

The Late Neogene sedimentary sequence consists of brownish calcareous siltstone and claystone, intercalated with packstone limestone based on Dunham [14], which is chalky and rich in planktonic foraminifera. This unit is comparable with Korem and Wardo formations according to Masria, *et al*. [9]. There is unconformity between the Late Neogene and the Early Neogene sedimentary sequence. Lithological changes from limestone to fine clastic carbonate rock that is rich in planktonic foraminifera are interpreted as subsidence due to sea level rise based on Permana [14]. The Quaternary sedimentary sequence consists of chalky coral limestone and some karstified sites. The limestone has a relatively coarse texture, granules >1 mm in size, consisting of coral and algal fragments, open fabric, and it has intergranular porosity. This unit is comparable with a Mokmer formation according to Masria, *et al.* [9]. It is thought to rest conformably on Korem and Wardo formations below.

4.2 Stratigraphic Model of Rock Resistivity

The stratigraphic model of rock resistivity was obtained from the correlation of the general rock resistivity (Table 1) against the stratigraphy of Biak and the surrounding area based on the field observations in Table 2. Stratigraphic unconformity is characterized by wavy lines in the contact with rock formations. There are four patterns of variation in rock resistivity in the sectional resistivity of Biak Island and the surrounding area, sorted from young to old rock based on the field observations compared to the regional geology of Biak based on Masria, *et al*. [9].

The Late Neogene to Quaternary sedimentary sequences show variations in resistivity, which decrease with depth, from 70,588 Ωm to 1,284 Ωm. Furthermore, patterns of variation in resistivity are indicated by the rock groups below. The Early Neogene sedimentary sequences show variations in resistivity, which increase with depth, from 28,506 Ωm to 42,538 Ωm. The changes in variation of resistivity imply that there are differences in physical rock

properties that cause the rock in this group to be more resistive. The Eocene basement found on Biak Island has a resistivity value that increases significantly when compared with the rock above it.

Table 3 Comparative results of the 1D inversion model of the stratigraphic model of rock resistivity.

No. point: **BK-13**

RES	Thick	depth	Formation
128.11	32.66	32.66	Quaternary
9.44	42.63	75.29	Quaternary
1.67	273.22	348.51	Quaternary
14.92	1,224.25	1,572.76	Late Neogene
1.15	946.18	2,518.94	Late Neogene
177.37	2,406.57	4,925.51	Early Neogene
29.27	8,102.44	13,027.95	S
114.44	10,000.00	23,027.95	?

No. point: **BK-14**

RES	Thick	depth	Formation
175.74	33.35	33.35	Quaternary
3.28	46.55	79.90	Quaternary
1.43	160.04	239.94	Quaternary
6.76	1,860.29	2,100.23	Late Neogene
2.12	1,277.69	3,377.92	Early Neogene
3,713.42	18,453.89	21,831.81	Igneous Base
41.74	31,865.89	53,697.70	?
12,103.64	10,000.00	63,697.70	?

No. point: **BK-25**

RES	Thick	depth	Formation
153.83	30.21	30.21	Quaternary
4.09	56.78	86.99	Quaternary
0.88	231.18	318.17	Quaternary
2.59	978.52	1,296.69	Late Neogene
8.54	1,679.02	2,975.71	Early Neogene
5.62	1,689.49	4,665.20	S
28.53	14,399.91	19,065.11	Igneous Base
167.32	10,000.00	29,065.11	?

No. point: **BK-02**

RES	Thick	depth	Formation
565.98	112.58	112.58	Quaternary
13.95	90.50	203.08	Quaternary
0.65	73.22	276.30	Quaternary
22.38	259.75	536.05	Late Neogene
2.78	374.36	910.41	Late Neogene
3.91	1,620.97	2,531.38	Early Neogene
68.76	18,003.68	20,535.06	Igneous Base
261.51	10,000.00	30,535.06	?

No. point: **BK-15**

RES	Thick	depth	Formation
604.39	118.15	118.15	Quaternary
23.89	86.39	204.54	Late Neogene
1.25	49.10	253.64	Late Neogene
4.92	380.65	634.29	Late Neogene
63.83	842.77	1,477.06	Early Neogene
10.33	1,000.26	2,477.32	Early Neogene
140.95	34,876.32	37,353.64	Igneous Base
178.28	10,000.00	47,353.64	?

No. point: **BK-16**

RES	Thick	depth	Formation
462.70	113.87	113.87	Late Neogene
19.38	69.78	183.65	Late Neogene
1.29	319.91	503.56	Late Neogene
8.81	1,289.03	1,792.59	Early Neogene
45.65	4,319.96	6,112.55	Igneous Base
429.74	23,626.91	29,739.46	?
56.68	21,130.45	50,869.91	?
691.35	10,000.00	60,869.91	?

No. point: **BK-17**

RES	Thick	depth	Formation
371.35	54.19	54.19	Quaternary
3,194.31	47.92	102.11	Late Neogene
36.78	87.71	189.82	Late Neogene
0.70	98.84	288.66	Late Neogene
5.01	1,072.03	1,360.69	Early Neogene
49.96	7,882.19	9,242.88	Igneous Base
148.71	47,007.00	56,249.88	?
484.06	10,000.00	66,249.88	?

No. point: **BK-18**

RES	Thick	depth	Formation
433.22	58.82	58.82	Quaternary
1,564.90	38.26	97.08	Late Neogene
44.77	114.49	211.57	Late Neogene
1.28	137.74	349.31	Late Neogene
9.40	692.56	1,041.87	Early Neogene
65.42	22,390.86	23,432.73	Igneous Base
114.62	37,787.23	61,219.96	?
46.04	10,000.00	71,219.96	?

No. point: **BK-19**

RES	Thick	depth	Formation
106.65	12.73	12.73	Early Neogene
6,020.95	69.36	82.09	Early Neogene
47.41	98.20	180.29	Early Neogene
4.72	515.31	695.60	Early Neogene
122.94	2,537.94	3,233.54	Igneous Base
25.62	3,191.80	6,425.34	?
95.30	35,436.25	41,861.59	?
387.39	10,000.00	51,861.59	?

No. point: **BK-20**

RES	Thick	depth	Formation
47.55	20.24	20.24	Early Neogene
17.55	19.19	39.43	Early Neogene
20.04	93.87	133.30	Igneous Base
7.59	439.20	572.50	Igneous Base
13.40	539.62	1,112.12	Igneous Base
86.74	5,240.75	6,352.87	Igneous Base
18.79	5,813.21	12,166.08	?
190.47	10,000.00	22,166.08	?

No. point: **BK-21**

RES	Thick	depth	Formation
27.64	16.50	16.50	Early Neogene
12.35	17.23	33.73	Early Neogene
46.51	38.95	72.68	Early Neogene
11.85	272.64	345.32	Early Neogene
5.45	228.97	574.29	Early Neogene
9.57	264.76	839.05	Igneous Base
38.97	16,893.67	17,732.72	Igneous Base
214.99	10,000.00	27,732.72	?

No. point: **BK-22**

RES	Thick	depth	Formation
156.83	89.39	89.39	Quaternary
12.40	52.44	141.83	Late Neogene
1.78	261.74	403.57	Late Neogene
13.25	2,128.79	2,532.36	Early Neogene
53.73	2,112.01	4,644.37	Igneous Base
15.41	2,773.48	7,417.85	Igneous Base
56.09	36,172.20	43,590.05	Igneous Base
245.90	10,000.00	53,590.05	?

No. point: **BK-23**

RES	Thick	depth	Formation
154.70	21.02	21.02	Quaternary
19.59	46.86	67.88	Quaternary
1.09	272.82	340.70	Quaternary
3.43	1,651.77	1,992.47	Late Neogene
7.56	4,079.83	6,072.30	Early Neogene
14.68	2,380.82	8,453.12	Igneous Base
51.66	49,231.21	57,684.33	Igneous Base
739.75	10,000.00	67,684.33	?

No. point: **BK-24**

RES	Thick	depth	Formation
66.12	34.27	34.27	Late Neogene
1.74	239.46	273.73	Late Neogene
6.66	1,175.21	1,448.94	Early Neogene
30.76	1,729.93	3,178.87	Igneous Base
19.56	3,208.01	6,386.88	Igneous Base
47.67	2,443.92	8,830.80	Igneous Base
138.00	19,007.64	27,838.44	Igneous Base
1,441.89	10,000.00	37,838.44	?

The oldest rock is the Pre-tertiary basement found on Supiori Island. This rock has a more conductive character because the resistivity value decreases significantly. The changes in rock resistivity found in the stratigraphic model of Biak Island indicate unconformities marked by differences in the physical properties of rock that is conductive or resistive.

A 1D inversion model was generated using Occam's inversion method. This method predicts the layers from the resistivity apparent curve to eight layers with varying resistivity values and thicknesses. Modeling into eight layers aims to obtain the maximum depth during the inversion process in order to increase

the data resolution. The comparative results of the 1D inversion model on the stratigraphic model of rock resistivity can be obtained qualitatively by observing the pattern of variation in rock resistivity controlled by formation thickness and rock distribution at the surface based on outcrop observations and regional stratigraphy according to Masria, *et al*. [9] (Table 3). The analysis was performed on data from each measurement point by Occam's inversion, with overall RMS errors ranging below 5%. The results of the inversion analysis show the pattern of significant changes in rock resistivity for five rock units.

The result of the 1D inversion model based on measurement data point BK-25 (Figure 6) shows a pattern of variation in resistivity that is divided into eight layers. Based on the order of the layers from top to bottom, correlated to Table 2, the first, second and third layers show a pattern of variation in resistivity with decreasing resistivity, interpreted as Late Neogene to Quaternary depositional sequences. Based on thickness, layers 1, 2 and 3 have a thickness of 30.21 m, 56.78 m, and 231.18 m respectively. Layers 4 and 5 show a pattern of variation in resistivity that increases compared to the layer above, interpreted as Early Neogene depositional sequences. These layers have a thickness of 978.52 m and 1,679.09 m respectively.

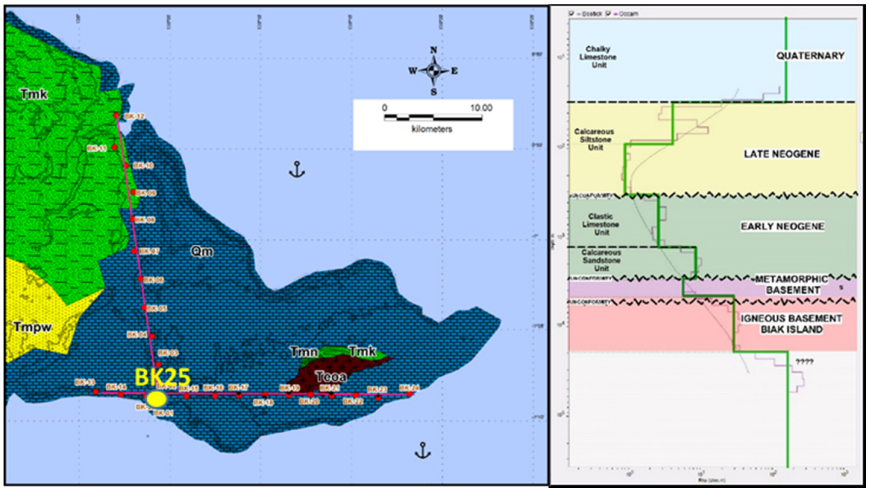

Figure 6 The results of the analysis of the stratigraphy model of rock resistivity in the 1D inversion model at measurement point BK-25.

Layer 6 shows a pattern of variation in resistivity that decreases towards the layer above, interpreted as Metamorphic Basement Supiori Island, which consists of metamorphic rock with a thickness of 1,689.49 m. Layer 7 shows a pattern of variation in resistivity that is significantly higher compared to the layer above and is interpreted as Igneous Basement Biak Island, which consists

of mafic-ultramafic igneous rock and volcanic rock with unknown thickness. Layer 8 cannot be interpreted because the thickness is unknown so it is considered a layer that continues downward.

4.3 Cross-section Analysis of 1D and 2D Resistivity

A cross-section analysis of 1D and 2D resistivity was conducted to determine the rock layers based on the different variations of resistivity and depth. The cross-sectional correlation of 1D resistivity of Biak Island against the stratigraphic model of rock resistivity (Table 2) produced several layers, which are differentiated based on the depth of each layer measured at each measurement point. The boundaries between the layers were qualitatively obtained based on differences in variation of resistivity, indicated by the wiggle and scale of the resistivity values. The lateral continuity of the layer was obtained by correlating the rock layers interpreted against 2D cross-sections along two lines: west-east and south-north, with RMS error for each line at 3.8% and 3.5%. Lateral discontinuities of the layers were interpreted as geological changes possibly caused by the geological structure.

The geophysical model of the 1D and 2D cross-sections resistivity on two MT lines in East Biak shows five layers, which can be interpreted based on the pattern of variation in resistivity as well as layer depth and thickness correlated with the Biak Island stratigraphy, as follows (Figure 7):

1. The first layer (above the yellow line) on the west-east and south-north line, characterized by a variation in resistivity from high to low, with a range of values from 1 to 604 Ωm and 1 to 6,530 Ωm. This layer is interpreted as a Quaternary sedimentary sequence, which consists of chalky coral limestone and some karstified sites. The layer is at a depth of ±350 m with an unknown continuity of layers from BK-17 to BK-22.
2. The second layer (above the green line) on the west-east and south-north line is characterized by a variation in resistivity from high to low and from low to high, with values ranging from 1 to 3,194 Ωm and 1 to 19,222 Ωm. This layer can be interpreted as Late Neogene sedimentary sequences. The layer is at a depth of ±2,500 meters with unknown continuity of layers on BK-19 to BK-22.
3. The third layer (above the purple or red line) on the west-east and south-north line is characterized by a variation in resistivity from low to high and from high to low, with values ranging from 2 to 6,021 Ωm and 1 to 250 Ωm. This layer is interpreted as an Early Neogene deposition sequence. The layer is at a depth of ±4,500 meters with continuity of layers from west to east and south to north.
4. The fourth layer (below the purple line or above the red line) on the west-east and south-north line is characterized by a variation in resistivity from

low to high and from high to low, with values ranging from 1 to 30 Ωm and >4,9 Ωm. This layer is interpreted as Metamorphic Basement Supiori Island at a depth of ±6,000 meters on the west and south side.

5. The fifth layer (below the red line) on the west-east and south-north line is characterized by a variation in resistivity from high to low and from low to high, with values ranging from 8 to 3,713 Ωm. This layer is interpreted as Igneous Basement Biak Island at a depth of ±7,000 m with continuity from west to east.

5 Discussion

Interpretation of the subsurface geology of East Biak was conducted based on the correlation of geophysical models against the rock distribution at the surface. The subsurface stratigraphy of East Biak was obtained from the results of a lateral distribution analysis of rock layers from 1D and 2D inversion modeling, the results of the stratigraphic modeling of rock resistivity values and geological maps. The geological structure was interpreted based on inconsistent variation and form of resistivity compared to regional geology and tectonic interpretations. The geological model of East Biak shows the presence of five layers of rock based on differences in resistivity in west-east and south-north cross sections (Figure 8).

The first layer, which is the oldest rock in eastern Biak, consists of Igneous Basement Biak Island, interpreted as Auwewa formation based on Masria *et al*. [9]. The layer is characterized by a pattern of variation in resistivity with more elevated values than in the layer above it. This formation is thought to be a Paleogene volcanic product originating from the island arc colliding with the northern part of the Australian continent, according to Gold *et al.* [6]. On the mainland of New Guinea, an Auwewa formation is the basement found in the Iroran and Apauwar wells in the Mamberamo area mentioned by Wachsmuth and Kunst in [15]. The second layer is interpreted as Metamorphic Basement Supiori Island, interpreted as a Korido formation. This rock is exposed in the southern part of Biak Island. In the cross-sectional resistivity, this layer has a very low variation of resistivity with unknown layer thickness. The rock outcrops show highly fractured and weathered rock so that they tend to be conductive. The relationship between the two formations is thought to be tectonic with the existence of thrust faults that led to the East Biak uplift.

The third layer is the Early Neogene sedimentary sequence in East Biak, which consists of the Wainukendi, Wafordori, and Napisendi formations. This layer is characterized by a pattern of variation in resistivity that tends to increase downward. The carbonate platform grew in the Early to Middle Miocene and is found not only on Biak Island but also in the Bintuni and Salawati basins. This

carbonate platform is part of the Limestone Guinea Group that was deposited at the same time in the western part of New Guinea according to Gold [16]. The collapsed structure is thought to be an impact of collision activity that occurred in the Paleogene. The tectonic regimes recorded on Biak Island are currently classified as extensive to transitive tectonics based on Saragih, *et al*. [8]. Tectonic activity as well as differences in the depositional environment imply an unconformable stratigraphic relationship with the rock layers below.

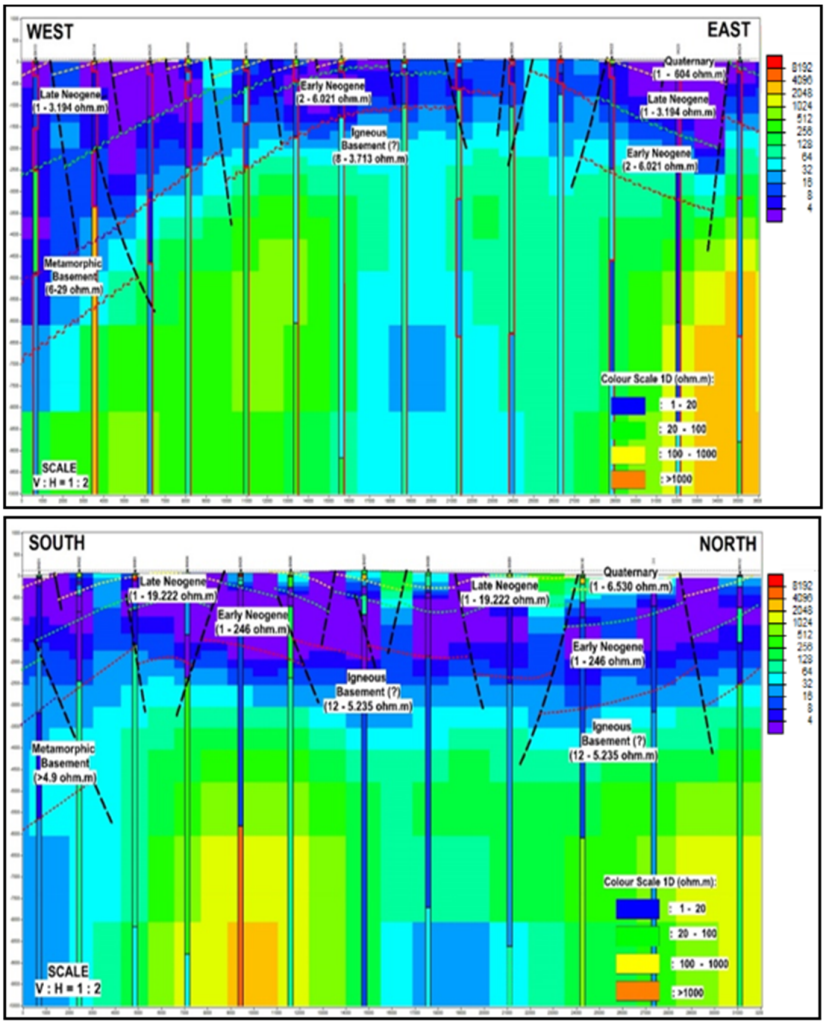

Figure 7 The west-east and south- north subsurface line of geophysical model in the Biak area and its surroundings shows the anticline form.

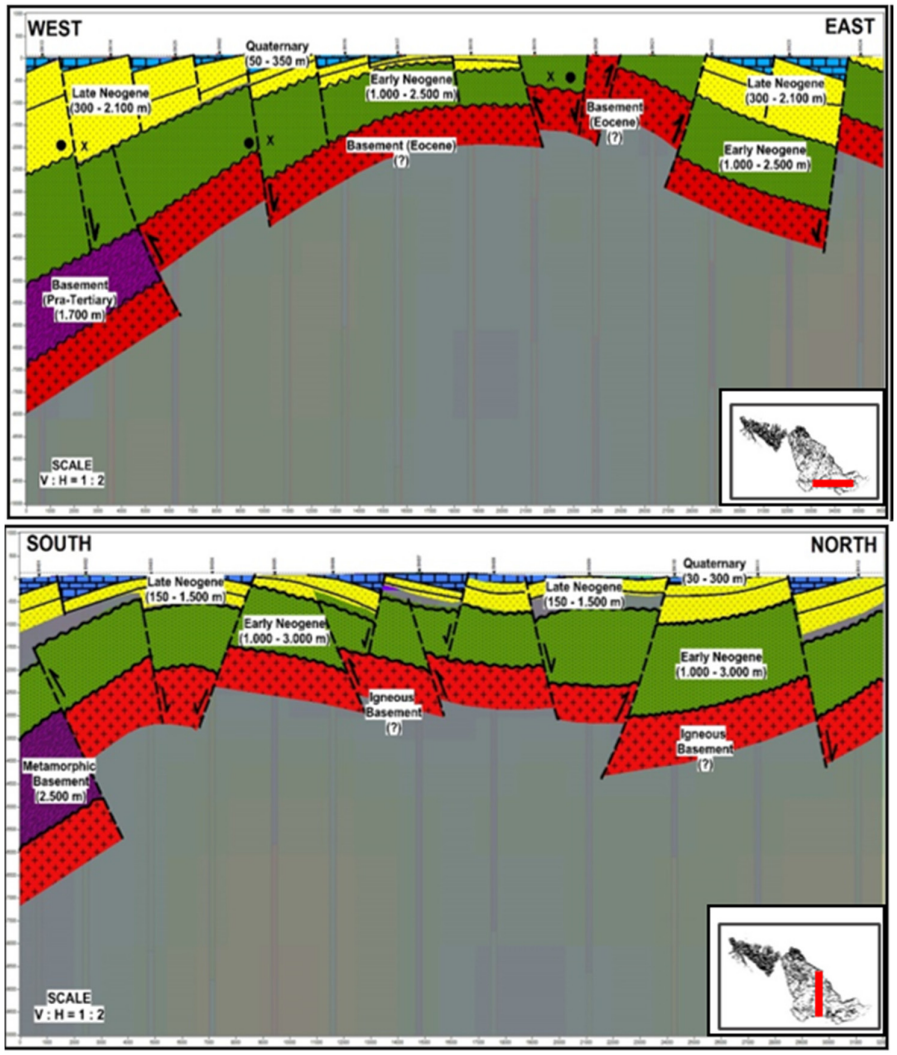

Figure 8 The subsurface geological model on the cross section of the west-east and south-north MT line in the East Biak area and its surroundings.

The fourth layer is a Late Neogene sedimentary sequence (Korem and Wardo formations). This layer is characterized by a pattern of variation with increasing resistivity going upwards. The rock deposition was caused by a relative sea level rise, resulting in the sinking of the carbonate platform in the Middle to Late Miocene based on Alviyanda, *et al*. [17]. Later uplift occurred with the deposition of Wardo formation in the Pleistocene. The variation of resistivity shows a relatively harmonious pattern, which increases up to the fifth layer,

which is a Quaternary sedimentary sequence (Mokmer formation). At present, there is a compressive uplift in eastern Biak Island as evidenced by Late Miocene to Holocene Korem, Wardo, and Mokmer formations, which became the mainland on Biak Island according to Saragih, *et al*. [8].

6 Conclusions

The East Biak stratigraphic model based on cross-sectional resistivity MT consists of five rocks units. The basement consists of Metamorphic Basement and Igneous Basement rock. The relationship between these two rock groups is a tectonic relationship that caused old rock to be between young rock. There are three overlying sedimentary sequences: Early Neogene, Late Neogene and Quaternary. There is an unconformable stratigraphic relationship between the Early Neogene sequence and the basement rock underneath it. Based on the MT resistivity cross-section, the Early Neogene deposition sequence has a thickness of 1,000 to 3,000 m, while the Late Neogene to Quaternary depositional sequence has a thickness of 180 to 2,450 m. These two sedimentary sequences have unconformable stratigraphic relationships that are characterized by changes in the rock depositional environment and differences in patterns of variation in rock resistivity.

Acknowledgment

The authors would like to thank the LPDP Scholarship program for funding this research and Geological Survey Center Bandung for supplying data.

Reference

[1] Dewey, J.F. & Bird, J.M., *Mountain Belts and the New Global Tectonics*, Journal of Geophysical Research, **75**, pp. 2625-2647, 1970.

[2] Milsom, J., Masson, D., Nichols, G., Sikumbang, N., Dwiyanto, B., Parson, L. & Kallagher, H., *The Manokwari Trough and the Western End of the New Guinea Trench*, Tectonics, **11**, pp. 145-153, 1992.

[3] Hall, R., *Cenozoic Geological and Plate Tectonic Evolution of SE Asia and the SW Pacific: Computer-based Reconstruction, Model and Animations*, Journal of Asian Earth Sciences, **20**, pp. 353-431, 2002.

[4] Cloos, M., Sapiie, B., Ufford, A.Q., Weiland, R.J., Warren, P.Q. & McMahon, T., *Collisional Delamination in New Guinea: The Geotectonics of Subducting Slab Breakoff,* The Geological Society of America Special Paper 400, 2005.

[5] Hill, K.C. & Hall, R., *Mesozoic-Cenozoic Evolution of Australia's New Guinea Margin in a West Pacific Context*, Geol. Soc. Australia Spec., Publ. 22, and Geol. Soc. America Spec. Pap., **372**, pp. 265-290, 2003.

[6] Gold, D.P., Hall, R., Burgess, P. & White, L., *Neogene Structural History of Biak and the Biak Basin, Eastern Indonesia,* South East Asia Research Group Poster, American Geophysical Union, Fall Meeting 2014, Abstract ID. T53C-4705, 2014.

[7] Bailly, V., Pubellier, M., Ringenbach, J.C., de Sigoyer, J. & Sapin, F., *Deformation Zone 'Jumps' in a Young Convergent Setting: The Lengguru Fold-and-Thrust Belt, New Guinea Island*, Elsevier, Lithos-02111, pp. 12, 2009.

[8] Saragih, R.Y., Junursyah, G.M.L., Badaruddin, F. & Alviyanda, *Structural Trap Modelling of The Biak-Yapen Basin as a Neogene Frontier Basin in North Papua,* Proceedings of the Indonesian Petroleum Association, 42nd Annual Convention and Exhibition, Jakarta, 2018.

[9] Masria, M., Ratman, N. & Suwitodirdjo, *Geological Map of Biak, Irian Jaya, Scale 1:250.000*, Center for Geological Research and Development, Bandung, 1981.

[10] Junursyah, G.M.L., *Final Report of Magnetotelluric Survey in Yapen-Biak Island and Its Surrounding Area, Papua,* Geological Survey Centre, Bandung, 2013. (Text in Indonesian and abstract in English); (Unpublished)

[11] Junursyah, G.M.L., Saragih, R.Y., Alviyanda, Suherman, T. & Suganda, A., *Final Report of 'WK MIGAS' Recommendation Study in Biak Basin and Its Surrounding Area, Internal Report of the Upstream Oil and Gas Survey Working Group*, Geological Survey Centre, Bandung, 2017. (Text in Indonesian and Abstract in English); (Unpublished)

[12] Alviyanda, Junursyah, G.M.L, Gumilar, I.S, & Mardiana, U., *Interpretation of Subsurface Structure in Tertiary Sediment Based on Magnetotelluric Data, South Buton area*, Proceedings of the Indonesian Petroleum Association, 38th Annual Convention and Exhibition, Jakarta, 2014.

[13] Dunham, R.J., *Classification of Carbonate Rocks According to Depositional Texture,* in: Ham, W.E., (eds.), Classification of Carbonate Rocks. Am. Association Petroleum Geologist Mem., **1**, pp. 108-121, 1962.

[14] Permana, A.K., *Final Report of Biak-Yapen Basin Stratigraphy Research, Papua,* Geological Survey Centre, Bandung, 2013. (Text in Indonesian and abstract in English); (Unpublished)

[15] Wachsmuth, W. & Kunst, F., *Wrench Fault Tectonics in Northern Irian Jaya*, Proceedings of the Indonesian Petroleum Association, 15th Annual Convention and Exhibition, Jakarta, pp. 371-376, 1986.

[16] Gold, D.P., *The Effect of Meteoric Phreatic Diagenesis and Spring Sapping on the Formation of Submarine Collapse Structures in the Biak Basin, Eastern Indonesia*, Indonesian Journal of Sedimentary Geology,

Minarwan, and Darman, H., eds., The Indonesian Sedimentologist Forum (FOSI), **41**, pp. 23-37, 2018.

[17] Alviyanda, Junursyah, G.M.L. & Saragih, R.Y., *Reservoir Potential of Neogene Rocks in the Biak Island and Its Surrounding Areas*, Indonesian Journal of Sedimentary Geology, Minarwan, and Darman, H., eds., The Indonesian Sedimentologist Forum (FOSI), **42**, pp. 33-42, 2019.